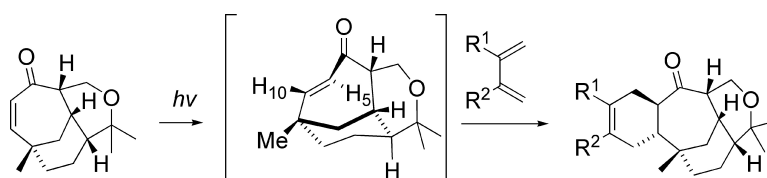


Mechanistic Studies of UV Assisted [4 + 2] Cycloadditions in Synthetic Efforts toward Vibsanin E

Joachim Nikolai, ystein Loe, Paulina M. Dominiak, Oksana O. Gerlitz, Jochen Autschbach, and Huw M. L. Davies

J. Am. Chem. Soc., **2007**, 129 (35), 10763-10772 • DOI: 10.1021/ja072090e • Publication Date (Web): 11 August 2007

Downloaded from <http://pubs.acs.org> on February 15, 2009



More About This Article

Additional resources and features associated with this article are available within the HTML version:

- Supporting Information
- Links to the 3 articles that cite this article, as of the time of this article download
- Access to high resolution figures
- Links to articles and content related to this article
- Copyright permission to reproduce figures and/or text from this article

[View the Full Text HTML](#)

Mechanistic Studies of UV Assisted [4 + 2] Cycloadditions in Synthetic Efforts toward Vibsantin E

Joachim Nikolai, Øystein Loe, Paulina M. Dominiak, Oksana O. Gerlitz,
Jochen Autschbach,* and Huw M. L. Davies*

Contribution from the Department of Chemistry, University at Buffalo, The State University of
New York, Buffalo, New York 14260-3000

Received March 24, 2007; E-mail: jochena@nsm.buffalo.edu; hdavies@buffalo.edu

Abstract: Quantum chemical DFT calculations at the B3LYP/6-31G(d) level have been used to study the stereochemical course of the photochemical cycloaddition of enone **9** with dienes. The observed products of this photochemically induced cycloaddition showed a stereoselectivity, which is opposite to what would be expected by FMO considerations. The quantum chemical calculations revealed that the unusual stereoselectivity of the reaction can be rationalized by assuming a stereospecific photochemical *cis*–*trans* isomerization of enone **9** to *trans* isomer **9a** followed by a thermal Diels–Alder reaction of the diene onto the highly reactive *trans* enone. The photochemical reaction step involves the selective formation of a twisted triplet intermediate, which accounts for the selectivity of the reaction.

Introduction

Recently we published synthetic efforts toward the diterpene vibsantin E¹ (**1**, Figure 1), a natural product first isolated in the late 1970s from *Viburnum odoratissimum* by Kawazu.² Since these pioneering investigations which elucidated the structures of vibsantin A–F the structural diversity of the vibsantin family has continued to grow and now contains structures such as 5-*epi*-vibsantin E (**2**) and vibsantin C (**3**) which are structurally closely related to **1**.^{2–7} Vibsantins show biological activities such as plant growth inhibition, cytotoxicity, and neurite outgrowth promoting activity.^{2,7–12}

Up to now there are no reported total syntheses of vibsantin E, although an epimer of vibsantin F has been synthesized as well as efforts toward the tricyclic core of vibsantin E have been described.^{3,4,6,7,13–15} We became interested in vibsantin E from

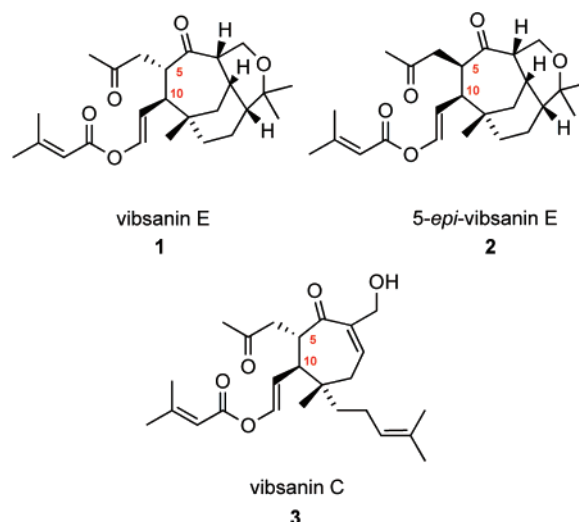
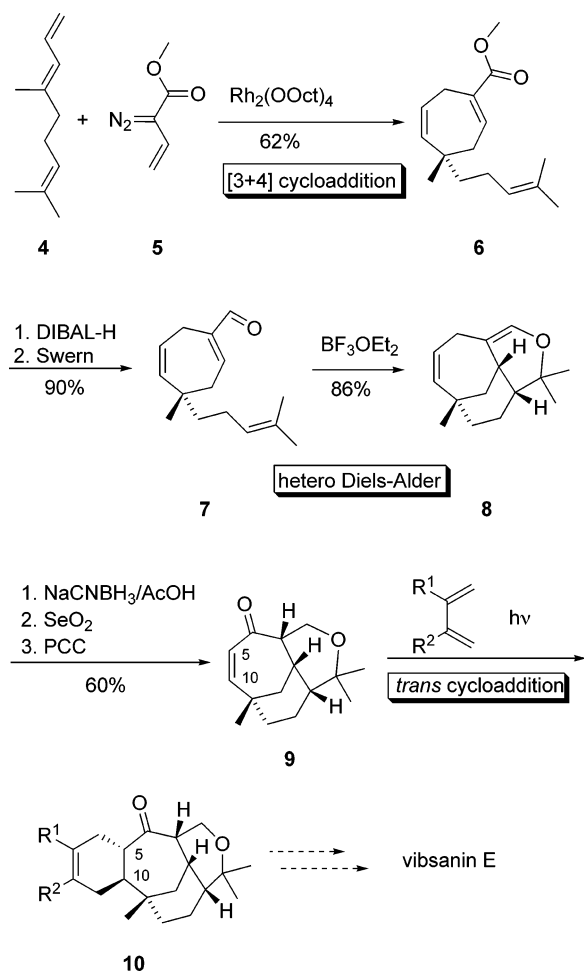


Figure 1. Vibsantin-type diterpenes.

a synthetic point of view because we realized that a rhodium catalyzed [4 + 3] cycloaddition between diene **4** and vinyl diazoacetate **5** would provide easy access to the seven-membered cycle found as a key element in the natural product (Scheme 1).¹ Moreover, we have demonstrated that the thus prepared cycloheptadiene **6** can serve as the starting material for a heteronuclear Diels–Alder reaction to form the tricyclic core **8** of vibsantin E on a multigram scale.¹ Further manipulations eventually allowed the synthesis of enone **9** which we planned to use as a substrate in yet another key cycloaddition reaction, a photochemically induced *trans* addition of an appropriately substituted diene onto the enone moiety of **9**. This reaction was expected to set up the relative stereochemistry required for the installment of the side chains at C5 and C10.¹ Our synthetic plan would therefore rely on three key cycloaddition reactions,

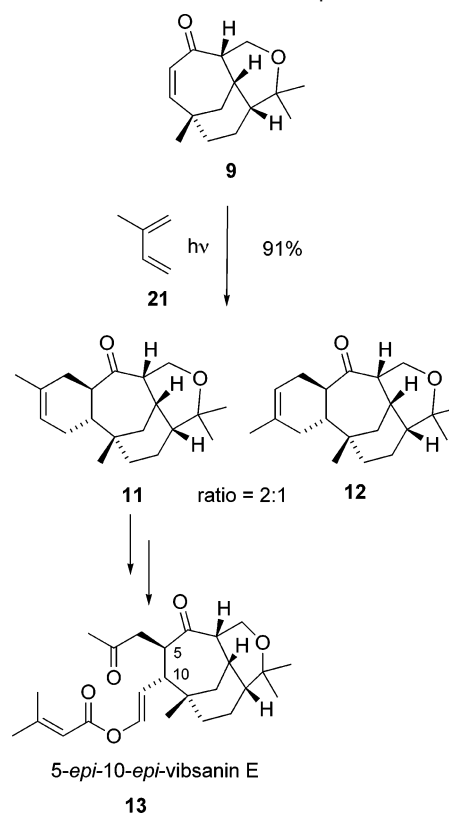
- (1) Davies, H. M. L.; Loe, O.; Stafford, D. G. *Org. Lett.* **2005**, *25*, 5561.
- (2) Kawazu, K. *Agric. Biol. Chem.* **1980**, *44*, 1367.
- (3) Fukuyama, Y.; Minami, H.; Takaoka, S.; Kodama, M.; Kawazu, K.; Nemoto, H. *Tetrahedron Lett.* **1997**, *38*, 1435.
- (4) Yuasa, H.; Makado, G.; Fukuyama, Y. *Tetrahedron Lett.* **2003**, *44*, 6235.
- (5) Fukuyama, Y.; Katsube, Y.; Kawazu, K. *J. Chem. Soc., Perkin Trans. 2* **1980**, 1701.
- (6) Fukuyama, Y.; Minami, H.; Kagawa, M.; Kodama, M.; Kawazu, K. *J. Nat. Prod.* **1999**, *62*, 337.
- (7) Fukuyama, Y.; Kubo, M.; Minami, H.; Yuasa, H.; Matsuo, A.; Fuji, T.; Morisaki, M.; Harada, K. *Chem. Pharm. Bull.* **2005**, *72*.
- (8) El-Gamal, A. A. H.; Wang, S.-K.; Duh, C.-Y. *J. Nat. Prod.* **2004**, *67*, 333.
- (9) Shen, Y.-C.; Prakash, C. V. S.; Wang, L.-T.; Chien, C.-T.; Hung, M.-C. *J. Chin. Chem. Soc.* **2003**, *50*, 297.
- (10) Duh, C.-Y.; El-Gamal, A. A. H.; Wang, S.-K. *Tetrahedron Lett.* **2003**, *44*, 9321.
- (11) Shen, Y.-C.; Prakash, C. V. S.; Wang, L.-T.; Chien, C.-T.; Hung, M.-C. *J. Nat. Prod.* **2002**, *65*, 1052.
- (12) Kubo, M.; Chen, I.-S.; Minami, H.; Fukuyama, Y. *Chem. Pharm. Bull.* **1999**, *47*, 295.
- (13) Fukuyama, Y.; Minami, H.; Takeuchi, K.; Kodama, M.; Kawazu, K. *Tetrahedron Lett.* **1996**, *37*, 6767.
- (14) Heim, R.; Wiedemann, S.; Williams, C. M.; Bernhardt, P. V. *Org. Lett.* **2005**, *7*, 1327.
- (15) Schwartz, B. D.; Tilly, D. P.; Heim, R.; Wiedemann, S.; Williams, C. M.; Bernhardt, P. V. *Eur. J. Org. Chem.* **2006**, 14.

Scheme 1. Key Steps in the Cycloaddition Approach toward Vibsanin E¹

which would eventually set up the main structural elements of vibsanin E (Scheme 1).¹

It is known in the literature that dienes are capable of undergoing a photochemical [4 + 2] cycloaddition to cyclic enones.^{16–18} A characteristic of these reactions is the *trans* addition of the diene across the enone. We were therefore curious to see if this methodology could provide a solution to our synthetic problem. We expected the photochemical cycloaddition to generate two anti products which would lead to the synthesis of both vibsanin E and its 5-*epi*-10-*epi* isomer from **9**. As we have communicated elsewhere,¹ under photochemical conditions, however, the reaction of **9** with isoprene afforded only compounds **11** and **12** in a 2:1 ratio and 91% combined yield. Ultimately, compound **11** could be successfully converted to 5-*epi*-10-*epi*-vibsanin E (Scheme 2).¹

To our surprise, none of the *trans* addition product with the correct configuration at C5 and C10 for vibsanin E was observed.¹ Furthermore, on the basis of Frontier Molecular Orbital (FMO) considerations of ground state cycloadditions and experimental work for a thermal cycloaddition reaction

Scheme 2. Photochemical Addition of Isoprene to Enone **9**

between cycloheptenones and isoprene, the cycloaddition reaction would be expected to form preferentially regioisomer **12**.^{19,20} In our case, however, the opposite regioselectivity was found.

Depending on their ring size, cyclic enones can undergo either a photochemical [2 + 2] reaction or a photochemically induced *cis*–*trans* isomerization.¹⁶ Unless otherwise constrained from undergoing *cis*–*trans* isomerization, enone rings of seven members or larger do not take part in excited-state cycloadditions but rather undergo rotational deactivation to form the *trans* isomer.¹⁶ *Trans* cycloheptenone can be generated photochemically via flash photolysis and is sufficiently long-lived to be observed and characterized by UV spectroscopy.²¹ Most prominently, the UV absorption band of the enone shifts from 220 nm in the *cis* isomer to 265 nm in the *trans* isomer, and the IR absorption for the C=O vibration is displaced from 1665 cm⁻¹ to 1715 cm⁻¹.^{17,18,21} Both findings show that geometric constraints in *trans* cycloheptenone cause deconjugation of the C=C and C=O double bonds. *Trans* cycloheptenone was found to react in the dark with alcohols to form products with the stereochemistry expected from a 1,4 addition across *trans* double bonds.^{22–25} Under identical conditions the *cis* isomer did not react with these nucleophiles.^{23,24} Quenching experiments demonstrated that the singlet *trans* isomer was the chemically active species.^{23,24} The use of *trans* cycloheptenone and its

(16) (a) Baldwin, S. W. In *Organic Photochemistry*; Padwa, A., Ed.; Marcel Dekker: New York, 1981; Vol. 5. (b) Dauben, W. G.; Van Riel, H. C. H. A.; Hauw, C.; Leroy, F.; Jousset-Dubien, J.; Bonneau, R. *J. Am. Chem. Soc.* **1979**, *101*, 1901. (c) Dauben, W. G.; Van Riel, H. C. H. A.; Robbins, J. D.; Wagner, G. J. *J. Am. Chem. Soc.* **1979**, *101*, 6383.

(17) Corey, E. J.; Tada, M.; LaMahieu, R.; Libit, L. *J. Am. Chem. Soc.* **1965**, *87*, 2051.

(18) Eaton, P. E.; Lin, K. *J. Am. Chem. Soc.* **1965**, *87*, 2052.

(19) Fleming, I. *Frontier Orbitals and Organic Chemical Reactions*; John Wiley & Sons: Chichester, 1976.

(20) Fringuelli, F.; Pizzo, F.; Taticchi, A.; Halls, T. D. J.; Wenkert, E. *J. Org. Chem.* **1982**, *47*, 5056.

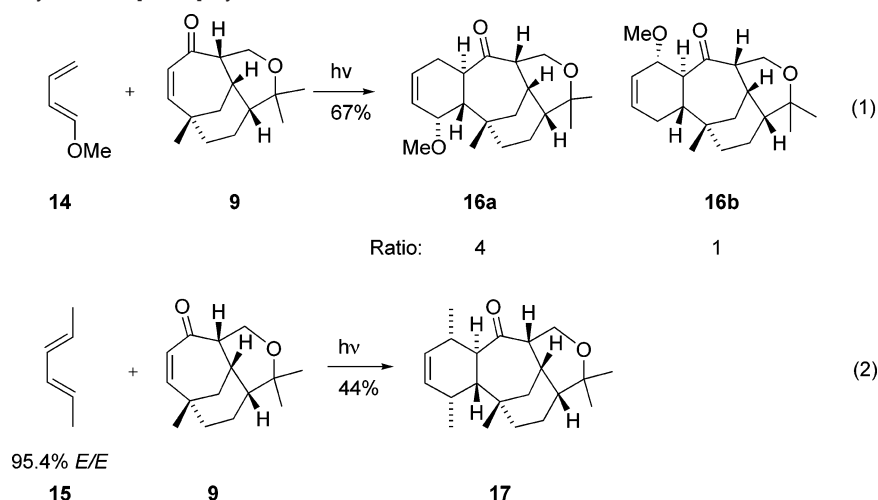
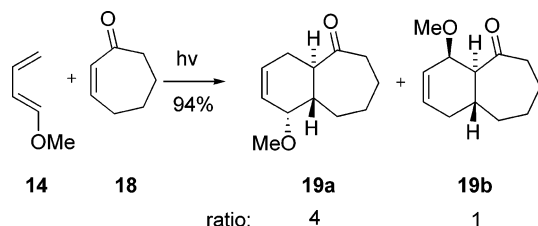
(21) Bonneau, R.; Fournier de Violet, P.; Jousset-Dubien, J. *Nouv. J. Chim.* **1976**, *1*, 31.

(22) Hart, H.; Dunkelblum, E. *J. Am. Chem. Soc.* **1978**, *100*, 5141.

(23) Noyori, R.; Kato, M. *Bull. Chem. Soc. Jpn.* **1974**, *47*, 1460.

(24) Noyori, R.; Watanabe, A.; Kato, M. *Tetrahedron Lett.* **1968**, 5443.

(25) Hart, H.; Chen, B.-I.; Jeffares, M. *J. Org. Chem.* **1979**, *44*, 2722.

Scheme 3. Photochemically Induced [4 + 2] Cycloadditions of Ketone **9****Scheme 4.** UV Promoted [4 + 2] Cycloaddition with Cycloheptenone (**18**)

benzoannulated derivatives in intermolecular [4 + 2] cycloadditions with cyclopentadiene and furan afforded diastereomers due to an *endo/exo* approach of the diene. To our knowledge the only report using an unsymmetrical diene describes the use of isoprene and only the regioisomer expected from FMO theory was observed for the Diels–Alder product.²⁶ An intramolecular variant was described by Dorr and Rawal.²⁷ Here, photoisomerization of the enone created a new element of chirality producing (as expected!) two diastereomeric enones, each capable of reacting with the diene moiety of the molecule in an *endo/exo* mode.²⁷ Thus, mechanistically, it is established that [4 + 2] cycloadditions to cycloheptenones under photochemical conditions are a two step process: First a photochemical *cis–trans* isomerization of the cycloenone occurs, which is then followed by a [4 + 2] or a Michael addition to the ground state of the *trans* enone.

In this paper we present the results of our study initiated to shed light on the unprecedented selectivity in the photochemical addition of enone **9** onto dienes. We were interested to find a rationale for (a) the diastereoselective photochemical *cis–trans* isomerization of **9**, which obviously produces only one *trans* isomer of **9** (*vide supra*), and (b) the unexpected (“non-FMO”) regioselectivity of the subsequent ground state Diels–Alder reaction.

Results and Discussion

In order to gather more experimental data, we decided to extend the photochemical reaction sequence shown in Scheme 2 by employing enone **9** as dienophile and 1-methoxy-1,3-butadiene (**14**) as well as 2,4-hexadiene (**15**) as dienes. Further,

as a simple model system, we chose the reaction of cycloheptenone (**18**) and 1-methoxy-1,3-butadiene (**14**). Scheme 3 shows the reactions of enone **9** with dienes **14** and **15**.

In all cases, the “anti”-Diels–Alder products are observed as the major products. From the ¹H NMR spectrum of the crude reaction mixture, a 4:1 ratio of **16a** to **16b** was determined (Scheme 3). The major product **16a** is the opposite regioisomer to that predicted for a conventional thermal Diels–Alder reaction.^{19,20} The only product that was isolable from the reaction of **9** with (*E,E*)-2,4-hexadiene was the anti-Diels–Alder product **17**. The structure of **16a** could be assigned unequivocally on the basis of NMR studies and a single crystal analysis²⁸ of **16a** (Figure 2): From the crystal structure it is apparent that the methoxy group is positioned at C9 and is pointing toward the concave side (“down”) of the tetracyclic structure. As is also seen from Figure 2, the hydrogen atom at C5 points toward the concave (“down”) side of **16a**, whereas the hydrogen atom at C10 occupies the less crowded convex face of the molecule.

Similar to the results of the reaction of enone **9** with diene **14**, the reaction of cycloheptenone (**18**) with **14** under the same conditions afforded cycloaddition products **19a** and **19b** in a 4:1 ratio (Scheme 4). In this case, however, the minor product **19b** was found to stem from an *endo* approach of the diene toward the enone. Compound **16b** requires an *exo* approach.

In all of the photochemical cycloadditions, *trans* fused compounds were produced but in the tetracyclic systems **16** and **17**, they were the opposite *trans*-fusion required for the vibsanin synthesis. Thus, we now turned our attention to *ab initio* calculations in order to gain further insight into the mechanistic details of the reaction (see “Computational Methods” for details). As shown in Scheme 5 for the reaction of **14** with cycloheptenone (**18**), we assumed for the reaction a two step process in which a photochemical *cis–trans* isomerization occurs first, which is then followed by a [4 + 2] cycloaddition (*vide supra*). An *endo/exo* approach of the diene allows for four different transition states for the reaction of *trans*-**18** with **14**. An *exo* approach leads to **TS19a** and **TS19c** whereas an *endo* approach leads to **TS19b** and **TS19d**. For comparison, we also calculated the energies of the transition states arising from the reaction of **14** with *cis*-**18** (**TS20a,b**).

(26) Shinozaki, H.; Arai, S.; Tada, M. *Bull. Chem. Soc. Jpn.* **1976**, *49*, 821.

(27) Dorr, H.; Rawal, V. H. *J. Am. Chem. Soc.* **1999**, *121*, 10229.

(28) X-ray crystallographic data have been submitted to the Cambridge Crystallographic Data Center, CCDC 242586 [Gerlits, O. O.; Coppens P. Private Communication].

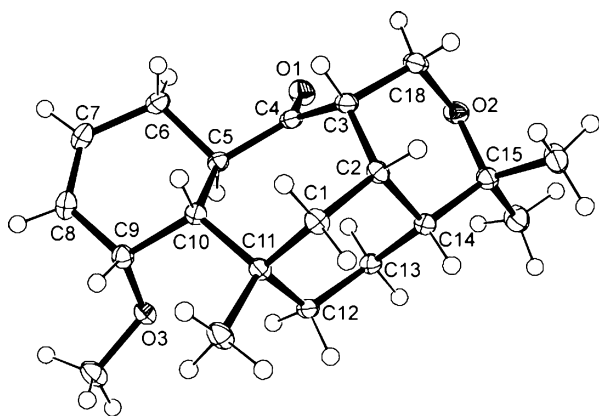


Figure 2. ORTEP plot²⁹ of **16a**. The ellipsoids of thermal vibration represent a 50% probability.

Table 1. Electronic Energies for *cis* and *trans* Cycloheptenone **18**

	<i>cis</i> - 18 $E_{\text{tot}}^a + \text{ZPE}^b$	<i>trans</i> - 18 $E_{\text{tot}}^a + \text{ZPE}^b$	<i>cis</i> - 18 → <i>trans</i> - 18 ΔE^c [kcal/mol]
B3LYP/6-31G(d)	-347.813 777	-347.758 487	+34.67
B3LYP/6-31+G(d)	-347.828 684	-347.773 180	+34.80
B3LYP/6-31G(d,p)	-347.828 670	-347.773 276	+34.74
B3LYP/6-311+G(d,p)	-347.914 621	-347.859 877	+34.33

^a Unit: hartree per molecule. ^b ZPE: zero-point energy in harmonic approximation; unscaled. ^c 1 hartree × N_A = 627.15 kcal/mol.

Table 2. Natural Population Analysis (NPA)³⁰ Atomic Charges and $\nu(\text{C}=\text{O})$ for *cis/trans*-**18**

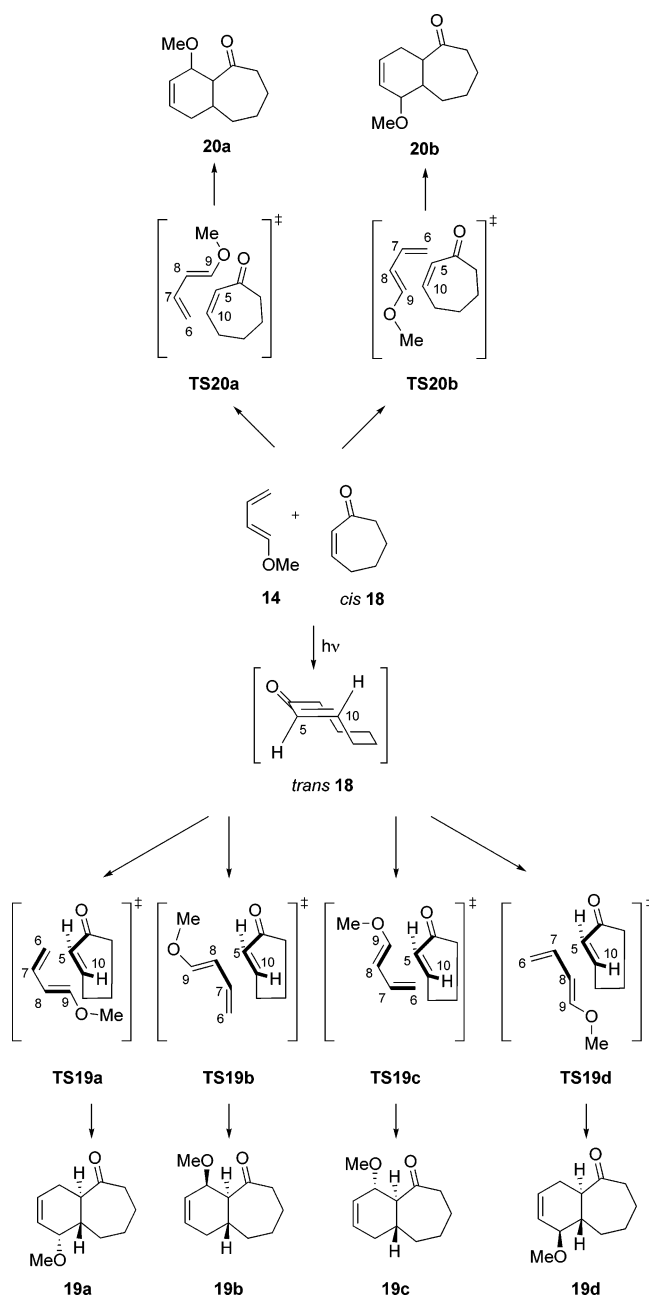
	<i>cis</i> - 18			<i>trans</i> - 18		
	C10	C5	$\nu(\text{C}=\text{O})^b$ [cm^{-1}]	C10	C5	$\nu(\text{C}=\text{O})^b$ [cm^{-1}]
B3LYP/6-31G(d) ^a	-0.146	-0.338	1749	-0.166	-0.313	1827
B3LYP/6-31+G(d) ^a	-0.142	-0.340	1720	-0.167	-0.311	1797
B3LYP/6-31G(d,p) ^a	-0.140	-0.342	1748	-0.171	-0.317	1827
B3LYP/6-311+G(d,p) ^a	-0.097	-0.306	1712	-0.125	-0.282	1793

^a Single-point calculations performed on structures optimized at same level of theory. ^b Wave numbers not scaled.

Table 1 summarizes the calculated electronic energies for *cis*- and *trans*-**18**. Clearly, the *trans* isomer is a high-energy structure, which lies 34 kcal/mol over the *cis* isomer (Table 1). As determined by experiment,^{17,18,21} the *trans* isomerization breaks the enone conjugation, shifting the carbonyl valence vibration to higher wave numbers. At all levels of theory this result is reproduced by the calculations (Table 2). Also, due to the missing enone conjugation, the carbon α to the carbonyl group (C5) becomes less negatively charged by an inductive effect of the carbonyl group (Table 2). Atom C10 on the other hand becomes more negatively polarized.

Comparing the possible transition states **TS19a–d** (Scheme 5, Figure 3), it is seen that the formation of **19a** is the favored process (Table 3). Clearly, by increasing the basis set size, the calculated ratios for **19a** and **19b** approach the experimentally determined ratios. Going from the 6-31G(d) basis set to the triple- ζ 6-311+G(d,p) basis set, the Boltzmann ratio of **TS19a** to **TS19b** improves from 70:30 to 82:18 thereby reproducing the observed ratios within experimental error (experimental ratios for the formation of **19a** vs **19b** were determined from ¹H NMR spectra of the crude reaction mixture). Using calculated free energies, neither the relative energetic order of the transition states nor the calculated ratios changed. For this reason, we will continue to discuss $E(0\text{ K})$ energies, which contain zero-point

Scheme 5



corrections throughout this study. Also, it has to be noted that calculated Gibbs free energies for large systems seem to be less reliable due to the fact that the harmonic oscillator model produces significant deviations.³¹ The formation of compounds emerging from **TS19c,d**, i.e., compounds **19c,d**, was not observed experimentally. For the Diels–Alder reaction of **14** with *cis*-**18**, **TS20a** would lead to **20a**, the product that would be expected based on FMO considerations and which was observed experimentally in a thermal Diels–Alder reaction.²⁰ This result further supports the validity of our theoretical approach. All transition states leading to actually observed products, i.e., **TS19a,b** and **TS20a** are concerted yet very asynchronous. For example at the 6-311+G(d,p) level of theory,

(29) Farrugia, L. J. *J. Appl. Crystallogr.* **1997**, *30*, 565.

(30) Reed, A. E.; Weinstock, R. B.; Weinhold, F. *J. Chem. Phys.* **1985**, *83*, 735.

(31) Würthwein, E.-U.; Hoppe, D. *J. Org. Chem.* **2005**, *70*, 4443.

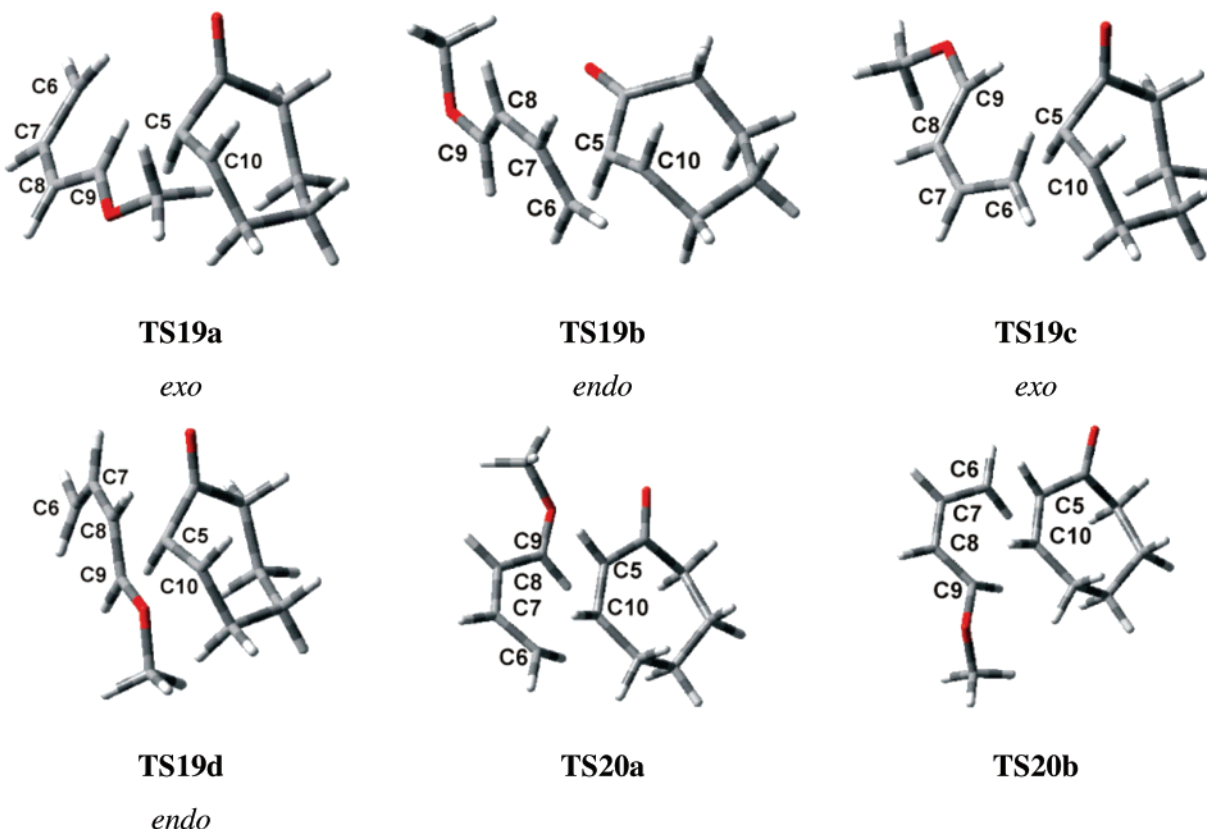


Figure 3. B3LYP/6-31G(d) optimized structures for **TS19a–d** and **TS20a,b**. *Endo/exo* refers to the approach of diene **14** relative to the twisted enone in *trans*-**18**. See Supporting Information for calculated electronic energies and zero-point energies.

Table 3. Transition State Energies for **TS19a–d** and **TS20a,b** Relative to *trans*-**18** and *s-cis*-**10** [kcal/mol]

	B3LYP/6-31G(d)	B3LYP/6-31+G(d)	B3LYP/6-31G(d,p)	B3LYP/6-311+G(d,p)
TS19a	3.06	5.33	3.02	5.88
TS19b	3.57	5.90	3.44	6.79
TS19c	4.63	7.17	6.45	7.79
TS19d	4.23	6.63	4.12	7.27
TS20a	21.24	23.84	23.06	24.78
TS20b	25.58	28.24	27.46	29.10
TS19a/TS19b^a	70:30	72:28	67:33	82:18

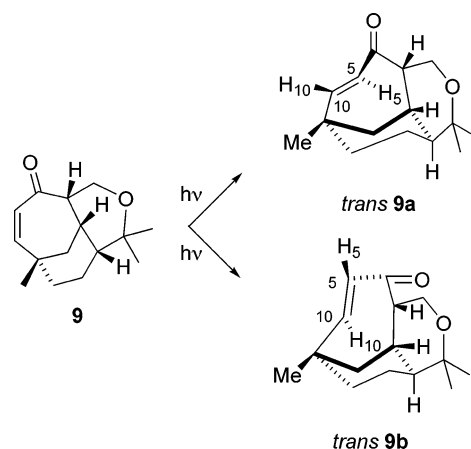
^a Ratio calculated for: $\text{TS19a/TS19b} = \exp(-\Delta E_{\text{TS}}/kT)$ with $T = 298$ K; ΔE_{TS} : energy difference between **TS19a** and **TS19b**.

the difference for the newly forming bonds between C5 and C9 and C10 and C6 in **TS20a** amounts to 0.65 Å with C5–C9 displaying the longer bonding distance. In **TS19b** the difference for these forming bonds is 0.55 Å. In **TS19a**, which is leading to the major products of the overall reaction, new bonds are formed between C5 and C6 and C9 and C10. Here, the distance between C9 and C10 is 0.44 Å greater than that between C5 and C6.

We next turned our attention to the photochemical cycloaddition of enone **9** with 1-methoxy-1,3-butadiene (**14**, Scheme 3) and isoprene (**21**, Scheme 2). Although we found a consistently improving Boltzmann ratio for the stereoselectivity of the cycloaddition of **14** with cycloheptenone (**18**) when going from the 6-31G(d) basis set to the triple- ζ 6-311+G(d,p) basis set, thus reproducing the experimental details (*vide supra*), we had to limit our studies for the significantly larger system of enone **9** with 1-methoxy-1,3-butadiene (**14**) and isoprene (**21**) to the 6-31G(d) basis set due to the high computational costs of these systems.

By using enone **9** as the dienophile in the photochemical cycloaddition with 1-methoxy-1,3-butadiene (**14**) and

Scheme 6



isoprene (**21**), not only the regioselectivity of cycloaddition to the *trans* isomer of **9** but also the fact that a *cis*–*trans* isomerization can generate two diasteric isomers *trans*-**9a** and *trans*-**9b** needs to be taken into account (Scheme 6).

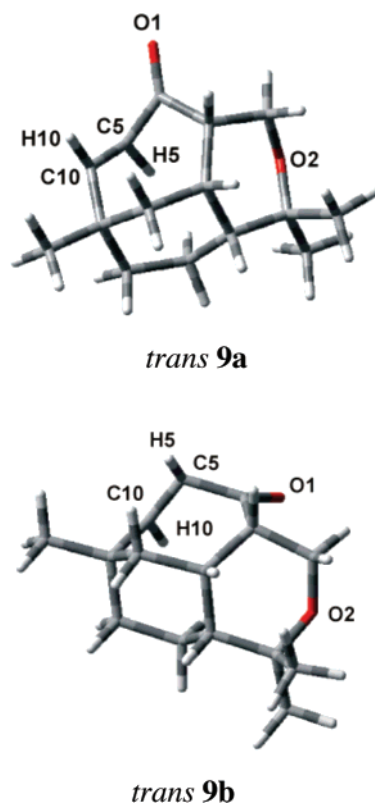


Figure 4. B3LYP/6-31G(d) optimized structures for *trans*-**9a,b**. See Supporting Information for calculated electronic energies and zero-point energies.

Calculations at the B3LYP/6-31G(d) level of theory locate the minimum structure for *trans*-**9a** 42.91 kcal/mol and for *trans*-**9b** 40.91 kcal/mol higher in energy than *cis*-**9** (Figure 4, Table 4). Both *trans* isomers can therefore be considered to be highly reactive in any subsequent cycloaddition reaction. Isomer *trans*-**9b** with H5 pointing toward the convex site and H10 toward the concave side of the tetracycle is favored thermodynamically by 2.00 kcal/mol (Boltzmann ratio *trans*-**9b**/*trans*-**9a** at 20 °C: 97:3). However, in all our reactions we only found cycloaddition products, which obviously have been formed from a [4 + 2] cycloaddition with *trans*-**9a** (Schemes 2 and 3). Isomers *trans*-**9a,b** both display chairlike conformations for the cyclohexyl and the tetrahydropyranyl rings fused to the cycloheptenone unit. This minimum conformation is also found in the single-crystal structure for **16a**. Possible boatlike conformers for the tetrahydropyranyl moiety were found to be minima, too, but with higher energy content (*cis*-**9** (boat): +3.6 kcal/mol; *trans*-**9a** (boat): +3.8 kcal/mol; *trans*-**9b** (boat): +2.6 kcal/mol). As for cycloheptenone (**18**, *vide supra*), carbon C5 in *trans*-**9a,b** is less negatively polarized as compared to the *cis* isomer and the C=O stretching vibration is shifted to higher wavenumbers (Table 4).

Table 4. B3LYP/6-31G(d) Electronic Energies, NPA³⁰ Atomic Charges for C5, C10, and $\nu(\text{C}=\text{O})$ for *cis*-**9** and *trans*-**9a,b**

	$E_{\text{tot}}^a + \text{ZPE}^b$	ΔE^c [kcal/mol] <i>cis</i> - 9 → <i>trans</i> - 9a	ΔE^c [kcal/mol] <i>cis</i> - 9 → <i>trans</i> - 9b	C5	C10	$\nu(\text{C}=\text{O})^d$ [cm ⁻¹]
<i>cis</i> - 9	-734.925 738			-0.325	-0.140	1736
<i>trans</i> - 9a	-734.857 338	+42.89		-0.306	-0.172	1823
<i>trans</i> - 9b	-734.860 532		+40.89	-0.303	-0.142	1824

^a Unit: hartree per molecule. ^b ZPE: zero-point energy in harmonic approximation; unscaled. ^c 1 hartree × $N_A = 627.15$ kcal/mol. ^d Wave numbers not scaled.

As supported by experimental evidence, isomer *trans*-**9a** has to be assumed to be the only isomer that is formed in the photochemical *cis*–*trans* isomerization of ketone **9**. Isomer *trans*-**9a** then undergoes a ground state [4 + 2] cycloaddition with 1-methoxy-1,3-butadiene (**14**) and isoprene (**21**) to yield compounds **11**, **12** (Scheme 2), and **16a,b** (Scheme 3). Figure 5 shows the quite asynchronous transition states **TS16a–d** which are found for a cycloaddition of **14** with *trans*-**9a** as well as **TS22a,b**, the transition states for a Diels–Alder reaction of *cis*-**9** with **14**.

Table 5 summarizes the calculated transitions state energies for **TS16a–d** and **TS22a,b**.

Transition state **TS16a**, which leads to **16a**, has the lowest energy. However, **TS16d** seems to be favored over **TS16b**. Thus, the calculations at this level of theory would predict the opposite configuration at C9 in **16b**. Comparing the energies for the transition states involving *cis*-**9**, **TS22a** would lead to a product carrying a methoxy substituent ortho to the carbonyl group in clear analogy to **TS20a**. However, we were unable to confirm this result experimentally, since all conditions reported to be successful in Diels–Alder reactions involving cycloheptenone derivatives^{20,32} failed in our hands. Figure 6 shows the two lowest energy, B3LYP-optimized, transition structures **TS11** and **TS12** leading to **11** and **12**, respectively (*cf.* Scheme 2). Although not seen in the final products, there is still the possibility of an *endo/exo* approach of the diene with respect to the convex shaped enone *trans*-**9a**. Both possible *endo* transition states leading to **11** or **12** are 0.57 kcal/mol, with respect to **TS11**, and 1.03 kcal/mol, with respect to **TS12**, higher in energy than the corresponding *exo* transition states. At the B3LYP/6-31G(d) level, an activation barrier of 5.46 kcal/mol was calculated for **TS11**. For **TS12**, the activation energy was found to be 5.58 kcal/mol. With these numbers, a 55:45 ratio would be predicted for the formation of **11** and **12**. Experimental results suggest a 2:1 ratio (Scheme 2).

To explain the unexpected selectivity in the *cis*–*trans* isomerization of enone **9**, we next examined closer the isomerization process for **9**. Our approach is based on experimental work on the photochemistry of enones and a theoretical study by Robb, Olivucci and co-workers examining the mechanism for excited-state potential surface crossings in acrolein.^{21,33–36} Spectroscopically, evidence could be found for a twisted triplet intermediate during the *cis*–*trans* isomerization of various enones including cycloheptenone and steroids.^{35,36} These twisted intermediates were found to be the reactive species which undergo efficient *cis*–*trans* isomerization upon intersystem crossing back to the singlet ground state.^{33,36} The angle of twisting of the double bond in these triplets and their lifetime vary with the rigidity of the molecule.^{33,36} For the triplet state of acrolein, experimental and computational studies suggest a 90° twist angle for the double bond.^{33,34} It was determined that

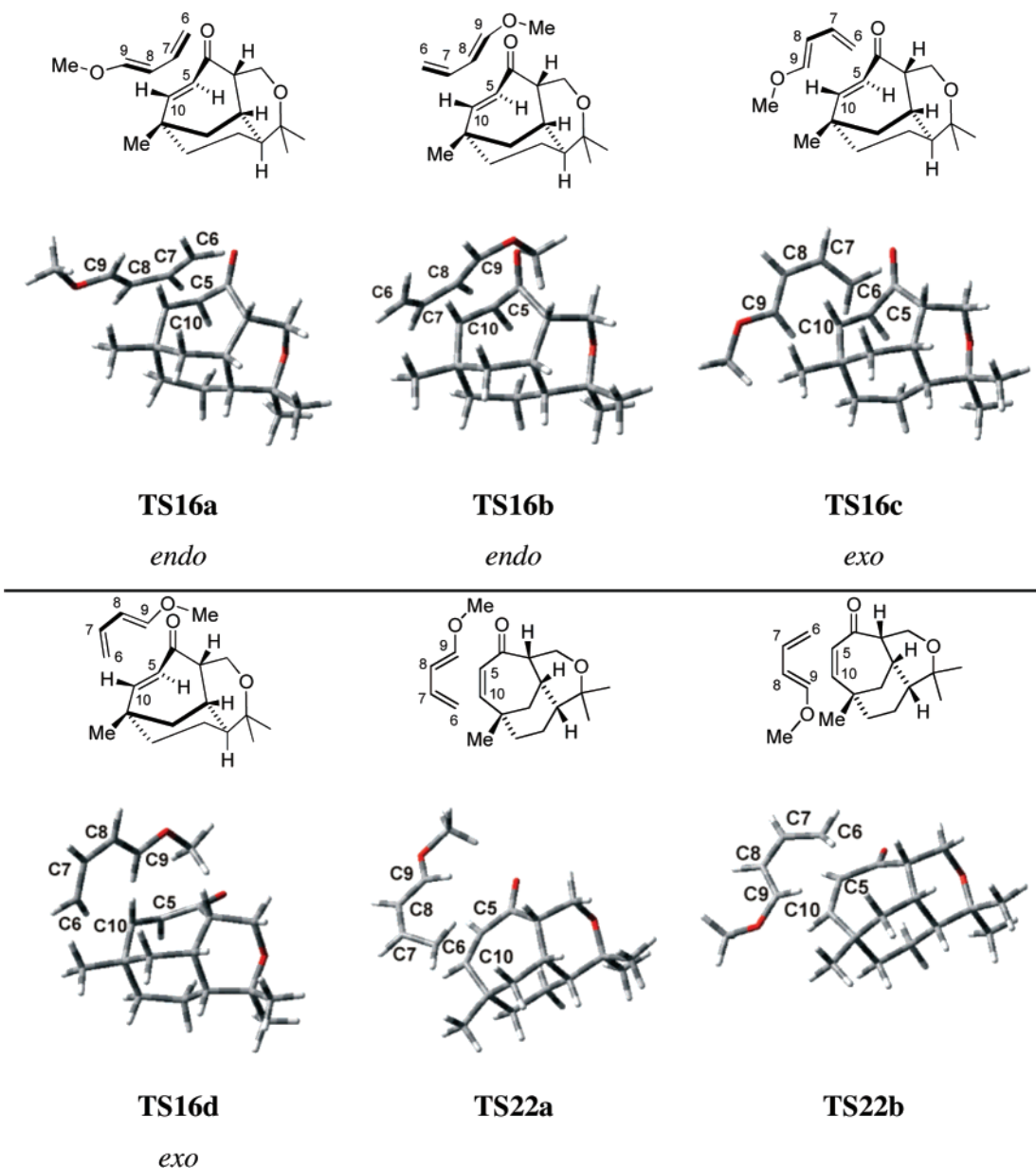


Figure 5. B3LYP/6-31G(d) optimized structures for **TS16a–d** and **TS22a,b**. *Endo/exo* refers to the approach of diene **14** relative to the twisted enone in *trans*-**9a**. See Supporting Information for calculated electronic energies and zero-point energies.

Table 5. B3LYP/6-31G(d) Electronic Energies for **TS16a–d** and **TS22a,b** Relative to *trans*-**9a** and *s-cis*-**14** [kcal/mol]

TS16a	TS16b	TS16c	TS16d	TS22a	TS22b
4.21	5.83	6.09	4.24	24.75	31.43

after photochemical excitation of the enone various electronic state crossing and recrossing processes lead to this triplet intermediate which is indeed the lowest energy triplet observed along the reaction coordinate of the isomerization.^{33,34} It should be emphasized that the acrolein mechanism is very complex, and a similar study on a more elaborate enone such as **9** is not

feasible. If we assume, however, that the isomerization of **9** involves a similar mechanism, then the differential stabilities of the involved triplet intermediates might lead to the selective formation of *trans*-**9a**. To this end we performed unrestricted B3LYP/6-31G(d) calculations on two diastereomeric, twisted structures of **9**. The structures are depicted in Figure 7.

In intermediate **23a** H5 points toward the concave side of the enone and this intermediate can therefore associate with enone *trans*-**9a**, whereas **23b** would lead to *trans*-**9b**. Compared to *cis*-**9**, the carbon–carbon bond lengths for the enone moiety are virtually equalized in the triplet states and the C=O double bond is slightly lengthened (Table 6). This is in agreement with reports on Complete Active Space Self-Consistent Field (CASSCF) structures for acrolein.³³ Based on the results from Table 6 it now becomes clear that **23a** is the more stable triplet intermediate in the *cis*–*trans* isomerization process of **9**. Triplet **23a** is found to be 4.62 kcal/mol more stable than **23b**, and we therefore explain the unexpected exclusive formation of *trans*-

(32) Fringuelli, F.; Pizzo, F.; Taticchi, A.; Wenkert, E. *J. Org. Chem.* **1983**, *48*, 2802.

(33) Reguero, M.; Olivucci, M.; Bernardi, F.; Robb, M. A. *J. Am. Chem. Soc.* **1994**, *116*, 2103.

(34) Becker, R. S.; Inuzuka, K.; King, J. *J. Chem Phys.* **1970**, *52*, 5164.

(35) Bonneau, R. *J. Am. Chem. Soc.* **1980**, *102*, 3816.

(36) Schuster, D. I.; Dunn, D. A.; Heibel, G. E.; Brown, P. B.; Rao, J. M.; Woning, J.; Bonneau, R. *J. Am. Chem. Soc.* **1991**, *113*, 6245.

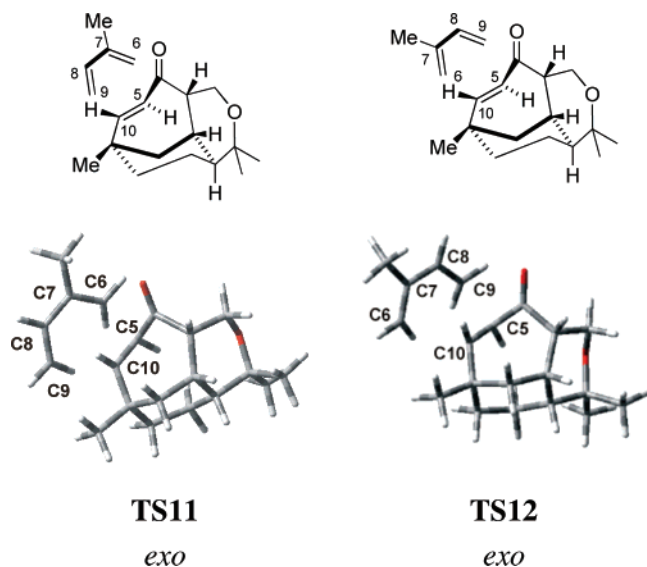


Figure 6. B3LYP/6-31G(d) optimized structures for **TS11** and **TS12**. See Supporting Information for calculated electronic energies and zero-point energies.

Table 6. UB3LYP/6-31G(d) Electronic Energies and Bond Lengths for Triplet **23a,b**

	23a	23b
$E_{\text{tot}}^a + \text{ZPE}^b$	-734.836 325	-734.828 962
ΔE^c [kcal/mol] 23a → 23b		+4.62
$\langle S^2 \rangle$	2.0144	2.0144
$d(\text{C5}-\text{C10})^d$ [Å]	1.455 23 (1.344 77)	1.456 16 (1.344 77)
$d(\text{C4}-\text{C5})^d$ [Å]	1.448 01 (1.487 78)	1.447 89 (1.487 78)
$d(\text{C4}-\text{O})^d$ [Å]	1.238 86 (1.226 80)	1.240 23 (1.226 80)
H5-C5-C10-H10 [deg]	87.690	77.895

^a Unit: hartree per molecule. ^b ZPE: zero-point energy in harmonic approximation; unscaled. ^c 1 hartree $\times N_A = 627.15$ kcal/mol. ^d Bond length for *cis-9* in parentheses.

9a by the stability difference of the involved twisted triplet structures. A significant difference for the dihedral bond H5-C5-C10-H10 is found between **23a** and **23b** (Table 6).

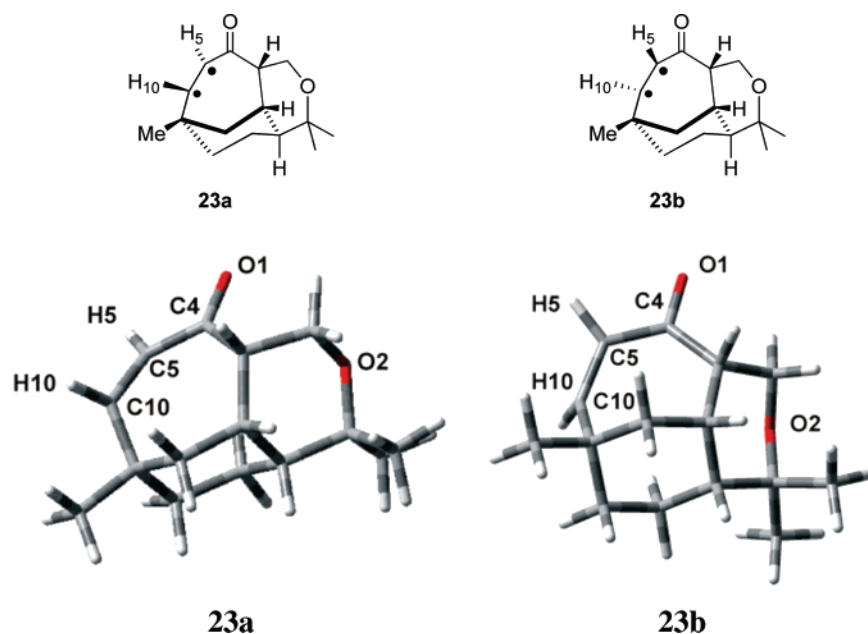
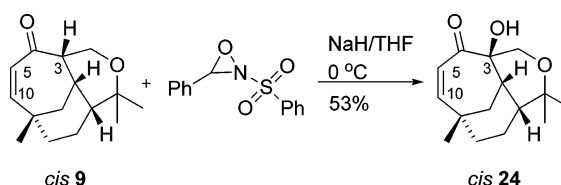


Figure 7. UB3LYP/6-31G(d) optimized triplet structures for triplets **23a,b**. See Supporting Information for calculated electronic energies and zero-point energies.

Scheme 7



Obviously, in **23a**, it is much easier to effect a twisting of the C=C double bond. It was found for acrolein that an efficient intersystem crossing (triplet \rightarrow singlet) leading to a *cis-trans* isomerization must occur at a fully twisted (90°) geometry of the enone.³³ It should be noted that, in systems where this 90° geometry cannot be fully reached, increased lifetimes of the triplet intermediates were found experimentally.³⁶ For **23a**, the value of the dihedral angle H5-C5-C10-H10 (87.690°) is virtually the same as that found by calculations at the same level of theory for acrolein (87.065°) and cycloheptenone (88.046°). Further, for the calculated triplet structures of acrolein and cycloheptenone, bond length equilibration for C5-C10 and C4-C5 is also observed (see Supporting Information for details).

In order to test these theoretical calculations, the synthetic studies were expanded to an additional tricyclic substrate. Introducing a hydroxy substituent at position C-3 in vibsantin E (**1**) leads to 3-hydroxy vibsantin E, another natural product.⁶ The required functionalization was easily accomplished on *cis-9* with Davis' oxaziridine³⁷ to yield *cis*-enone **24** (Scheme 7).

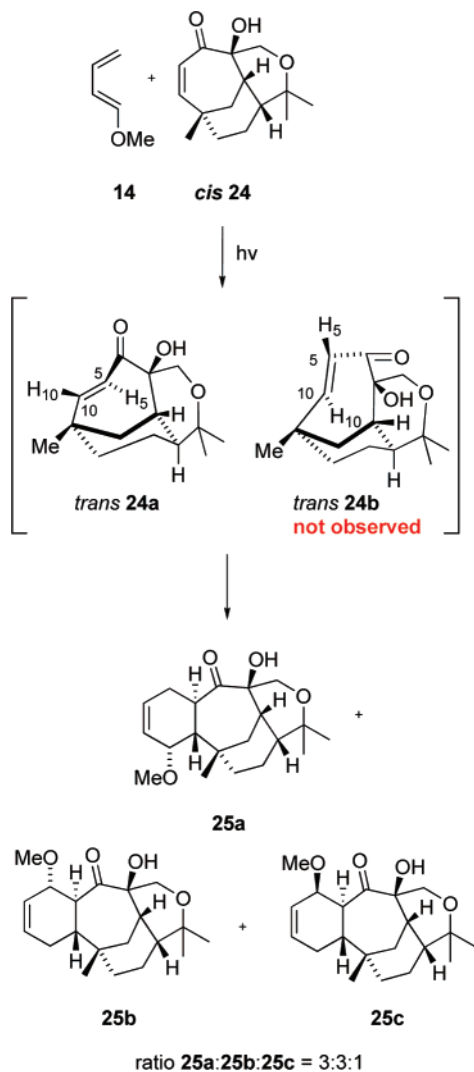
We used *cis-24* to test our mechanistic hypothesis and reacted **24** with 1-methoxy-1,3-butadiene (**14**) in a photochemically assisted [4 + 2] cycloaddition (Scheme 8). To our great satisfaction, we found that products **25a,b,c** are apparently produced from only one photochemically formed *trans* isomer.

Table 7 summarizes the results of the calculations for *trans-24a,b* (see Supporting Information for pictures of the calculated structures). Isomer *trans-24a* is found to be thermodynamically favored. Looking at the stereochemistry of products **25a-c** it

Table 7. B3LYP/6-31G(d) Electronic Energies for *trans*-**24a,b**

	$E_{\text{tot}}^a + \text{ZPE}^b$	ΔE^c [kcal/mol] <i>cis</i> - 24 \rightarrow <i>trans</i> - 24a	ΔE^c [kcal/mol] <i>cis</i> - 24 \rightarrow <i>trans</i> - 24b
<i>cis</i> - 24	-810.133 129		
<i>trans</i> - 24a	-810.070 716	39.14	
<i>trans</i> - 24b	-810.066 896		41.54

^a Unit: hartree per molecule. ^b ZPE: zero-point energy in harmonic approximation; unscaled. ^c 1 hartree $\times N_A = 627.15$ kcal/mol.

Scheme 8

becomes apparent that *trans*-**24a** is also the isomer that has to be formed in the photochemical *cis*-*trans* isomerization. The greater stability of *trans*-**24a** can be attributed to a stabilizing hydrogen bond between the carbonyl function of the *trans* enone and the hydroxy group at C3 (see Supporting Information).

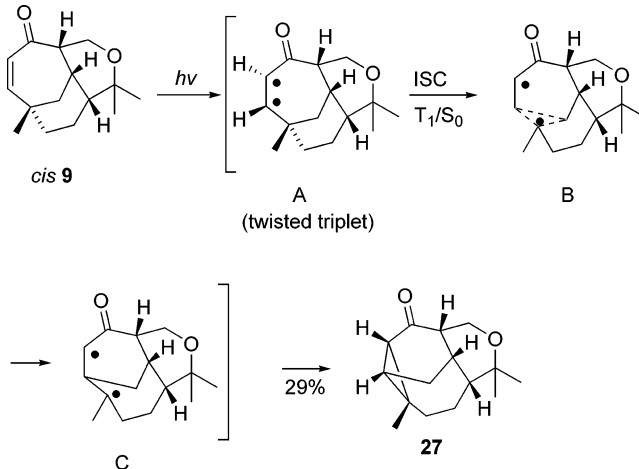
Figure 8 shows the UB3LYP optimized structures for triplet structures **26a,b**, which are postulated as intermediates in the *cis*-*trans* isomerization of **24**. Structure **26a** leads to *trans*-**24a**, which is the *trans* isomer found to be chemically reactive in the cycloaddition reaction with **14**.

As seen from Table 8, **26a** is stabilized relative to **26b** by 1.73 kcal/mol. This is in full agreement with our assumption (*vide supra*) that the observed *cis*-*trans* isomerization proceeds *via* the more stable triplet intermediate.

Table 8. UB3LYP/6-31G(d) Electronic Energies and Bond Lengths for Triplet **26a,b**

	26a	26b
$E_{\text{tot}}^a + \text{ZPE}^b$	-810.043 237	-810.040 476
ΔE^c [kcal/mol] 26a \rightarrow 26b		1.73
$\langle S^2 \rangle$	2.0076	2.0138
$d(\text{C5}-\text{C10})^d$ [Å]	1.455 58 (1.344 52)	1.453 19 (1.344 52)
$d(\text{C4}-\text{C5})^d$ [Å]	1.445 21 (1.474 38)	1.438 23 (1.474 38)
$d(\text{C4}-\text{O})^d$ [Å]	1.240 43 (1.230 38)	1.245 49 (1.230 38)
$\text{H}_\alpha-\text{C5}-\text{C10}-\text{H}_\beta$ [deg]	87.037	82.555

^a Unit: hartree per molecule. ^b ZPE: zero-point energy in harmonic approximation; unscaled. ^c 1 hartree $\times N_A = 627.15$ kcal/mol. ^d Bond length for *cis*-**24** in parentheses.

Scheme 9

Finally, further evidence for our hypothesis that the photochemical *cis*-*trans* isomerization of **9** proceeds via a triplet state was provided upon irradiation of *cis*-**9** in CH_2Cl_2 in the absence of any diene: It has been reported in the literature that cycloenones which are able to undergo a *cis*-*trans* isomerization normally dimerize to form cyclobutane derivatives if no trapping reagents, e.g., dienes, are present.³⁸ Their formation can be rationalized by assuming a *cis*-*trans* isomerization of one molecule of the enone followed by a [2 + 2] cycloaddition of the thus formed reactive *trans* isomer with one molecule of the *cis* isomer of the enone, i.e., one molecule of the cycloenone that has not yet undergone the photochemically induced *cis*-*trans* isomerization.³⁸ In our case, however, the isolated compound was **27**, whose structure was confirmed by X-ray crystallography³⁹ (Scheme 9). The dimerization products of one molecule of *trans*-**9** with one molecule of *cis*-**9** were not observed. We assume that the expected dimerization process was not observed due to the steric demand of enone **9**. The formation of rearrangement product **27** can be explained by a lumiketone-type rearrangement of *cis*-**9** in which a photochemically excited ${}^3(\pi-\pi^*)$ state (Scheme 9, **A**) is assumed to undergo intersystem crossing (ISC) back to the ground state, upon which a reorganization of bonds can be formulated (see structures **B** and **C**) which ultimately leads to the lumiketone-type rearrangement product **27**.⁴⁰ In the lumiketone sequence,

(38) Bunce, R.; Taylor, V. L.; Holt, E. M. *J. Photochem. Photobiol. A: Chem.* **1991**, *57*, 317.

(39) X-ray crystallographic data have been submitted to the Cambridge Crystallographic Data Center, CCDC 270719 [Dominiak, P. M.; Coppens, P. Private Communication].

(40) Schuster, D. I.; Brown, R. H.; Resnick, B. M. *J. Am. Chem. Soc.* **1978**, *100*, 4504.

(37) Davis, F. A.; Chattopadhyay, S.; Towson, J. C.; Lal, S.; Reddy, T. *J. Org. Chem.* **1988**, *53*, 2087.

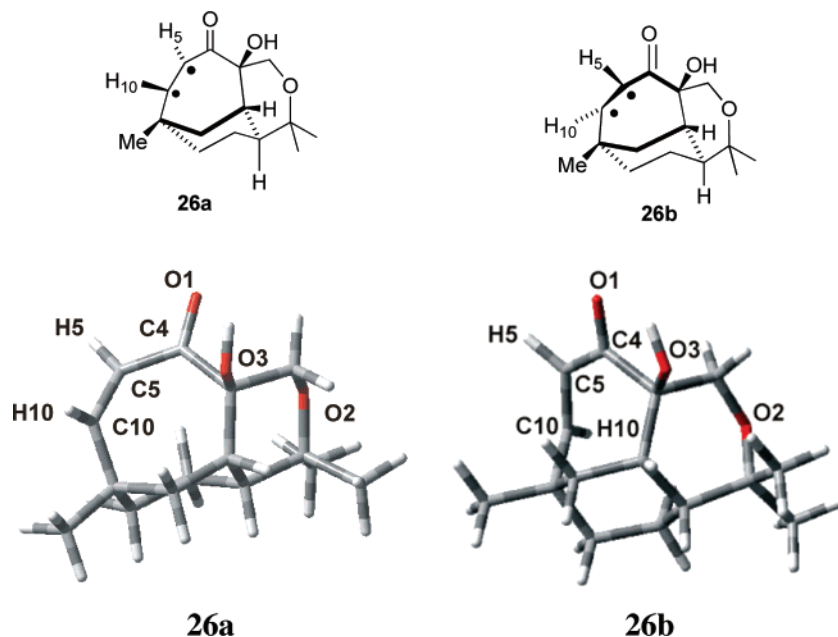


Figure 8. UB3LYP/6-31G(d) optimized triplet structures for triplets **26a,b**. See Supporting Information for calculated electronic energies and zero-point energies.

the excited state **A** is assumed to be a twisted triplet.^{40,41} In the context of our study it is thus crucial to note that for lumiketone-type rearrangements a twisted triplet intermediate is also assumed (compare structure **A** and **23a**, **26a**), thereby supporting the mechanism we propose for the *trans*-selective photochemical [4 + 2] cycloaddition of dienes to enones **9** and **24**.

Conclusion

In this paper we gave a detailed mechanistic account of a photochemical assisted [4 + 2] cycloaddition of dienes to tetracyclic enones, which we utilized in a crucial step in our synthesis toward vibsanan E and potential analogues. The unusual selectivity observed in this reaction can be rationalized by assuming a stereoselective photochemical *cis*–*trans* isomerization of the enones followed by a thermal Diels–Alder reaction of the diene onto a highly reactive *trans* enone. We propose the photochemical isomerization to the *trans* enone involves the selective formation of one of two possible twisted triplet intermediates, which accounts for the stereoselectivity of the overall reaction. The formation of a lumiketone-type rearrangement product from one of the substrates in the absence of dienes further supports the assumption of a twisted triplet being involved in the photochemical *cis*–*trans* isomerization.

Computational Methods

Semiempirical (AM1⁴²) and density functional theory (DFT, B3LYP functional⁴³) methods using Gaussian type basis sets as implemented in the Gaussian 98 program package were used for geometry optimizations.⁴⁴ Default convergence criteria for electronic structure, geometries, and transition states as implemented in the program were applied. Initial guess geometries for the reported transition states were found by optimizing a complex of the diene and the enone in which the distances

C6 (diene)–C10 (enone) and C9 (diene)–C5 (enone) were fixed at 2.00 Å, and all other parameters were optimized without geometry constraints at the AM1 level of theory. Next, all geometry constraints were dropped, and an AM1 transition state search was performed. The AM1 optimized structures (minima as well as transition states) were used as input structures for the density functional theory (DFT) calculations with Gaussian-type basis sets as listed in the tables in the section “Results and Discussion”. Reported minimum structures were confirmed by analytic frequency calculations having no imaginary harmonic vibrational frequencies. All transition states were confirmed as well having exactly one imaginary normal mode corresponding to the formation of the C–C bonds. Moreover, transition states were characterized by an intrinsic reaction coordinate (IRC) search.^{45–47} Calculated harmonic zero-point energies and harmonic frequencies are reported unscaled as the reported⁴⁸ scaling factors are close to one for the DFT methods used in the present study. Corrections for basis set superposition errors (BSSE) are not included. Population analysis was performed with the program package NBO 3.1⁴⁹ as implemented in Gaussian 98.

Acknowledgment. Financial support of this work by the National Science Foundation (CHE-0350536) is gratefully acknowledged. J.N. thanks the Deutsche Forschungsgemeinschaft (DFG) for a postdoctoral fellowship. The authors thank Thomas Nau at the Universitätsrechenzentrum Ulm for local implementation of Gaussian 98 and generous allocation of CPU time.

Supporting Information Available: Experimental details; physical data and ¹H NMR spectra for compounds **16a,b**, **17**, **19a,b**, **24**, **25a–c**, and **27**; stereochemical assignments for **16a,b**, **17**, **19a,b**, and **25a,b**; ORTEP-plot for **27**; bond length tables and Cartesian coordinates for calculated structures. This material is available free of charge via the Internet at <http://pubs.acs.org>.

JA072090E

(41) Reguero, M.; Bernardi, F.; Olivucci, M.; Robb, M. A. *J. Org. Chem.* **1997**, *62*, 6897.
 (42) Dewar, M. J. S.; Zoebisch, E. G.; Healy, E. F.; Stewart, J. J. *J. Am. Chem. Soc.* **1985**, *107*, 3902.
 (43) Becke, A. D. *J. Chem. Phys.* **1993**, *98*, 5648.
 (44) Frisch, M. J., et al. *Gaussian 98*, revision A.11; Gaussian Inc.: Pittsburgh, PA, 2001.

(45) Gonzales, C.; Schlegel, H. B. *J. Phys. Chem.* **1990**, *94*, 5523.
 (46) Gonzales, C.; Schlegel, H. B. *J. Chem. Phys.* **1989**, *90*, 2154.
 (47) Foresman, J. B.; Frisch, A. *Exploring Chemistry with Electronic Structure Methods*; Gaussian Inc.: Pittsburgh, PA, 1993.
 (48) Koch, W.; Holthausen, M. C. *A Chemist's Guide to Density Functional Theory, 2nd Edition*; Wiley-VCH: Weinheim, 2001.
 (49) Glendening, E. D.; Reed, A. E.; Carpenter, J. E.; Weinhold, F. *Gaussian NBO*, version 3.1